A Sound Approach for Stereo Three-line Scanner's Images

J. Wu
Center for Space and Remote Sensing Research (CSRSR)
National Central University, Chung-Li,
Taiwan, Republic of China

Abstract

A digital three-line scanner has three CCD linear arrays on its focal plane. The CCDs are placed perpendicular to flight direction and separated by an image base. This allows the scanner to image stereoscopically earth's terrain of interest. MEOSS now under construction and MAPSAT once proposed are mentioned as examples. The objectives in geometric analyses of stereo images from three-line scanners are derivations of Digital Terrain Models and of positions and attitudes along a flight path. Because of dynamic behaviors in forward motions of a sensor carrier, position and attitude parameters are functions of time. If the time-dependent parameters are realistically modelled, very accurate results can be obtained in an estimation process.

In the present report, the method of linear prediction is adopted as models for the parameters of exterior orientation. Simulation studies show that root mean square errors at check points are at the level of 1/3 of a pixel, when using only 3 GCPs in a strip 720 km long and 240 km wide.

Keywords: Geometric aspects with three-line scanners, Models for time-dependent parameters, Parameter estimation, Simulation, Accuracy at known exposure stations and at check points

1. Introduction

A stereo three-line scanner uses three CCDs on its focal plane for data acquisition. At any given time, only three line profiles can be scanned across-track. The ability to scan strips relies upon forward movement of sensor carriers. If a flight is disturbed by environmental factors, geometric (and radiometric) quality of the stereoscopic images taken by a three-line scanner is deteriorated. Generally, points on a terrain surface are at different elevations. These result partly in radial displacements of points in image space along CCD-sensors and partly in changes of cycle numbers associated with the image points.

Now, all orientation parameters and point coordinates should be determined in a combined manner in an aero-triangulation, applying conjugate image points correlated in stereo image pairs. Computation techniques are well developed in the conventional analytical photogrammetry. The method of least squares adjustment,
- point-referred formulations of the system of (partially reduced) normal equations and
- additional sub-systems of error equations used to express precision measures of reference data like known coordinates of GCPs

are not unfamiliar to modern photogrammetrists.

2. Models for time-dependent parameters

In any geometric evaluation of scanner's imagery, collinearity conditions contain the parameters of exterior orientation which are time-dependent, as shown in the following equation with the sub-index j,

$$f_{xy} = f(x_i', y_i', x_p, y_p, c, x_{O_j}, y_{O_j}, z_{O_j}, \omega_j, \varphi_j, \kappa_j, x_i, y_i, z_i)$$

where x_i', y_i' = measured coordinates of image point i

x_p, y_p, c = parameters of interior orientation

x_i, y_i, z_i = coordinates of point i in object space.

Each exposure station has its own set of positions x_{O_j}, y_{O_j}, z_{O_j} and attitudes ω_j, φ_j, κ_j, when a three-line picture is taken. If every station is treated discretely, this leads undoubtedly to a large number of unknowns.
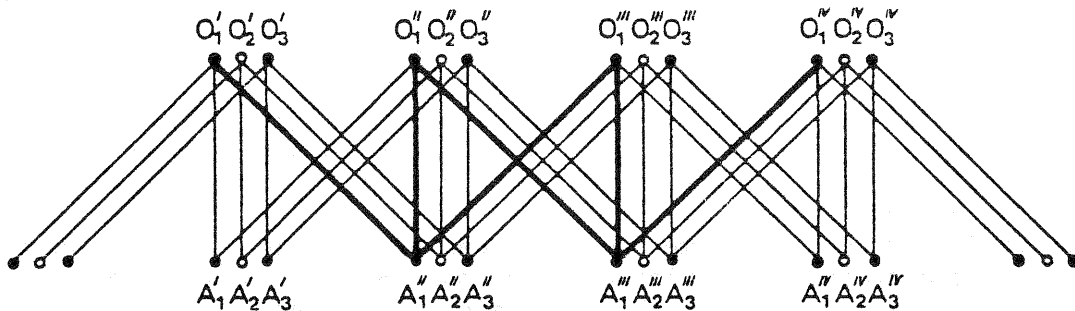

Figure 1. Geometric relationship between exposure stations $O_1' \ldots O_3^{IV}$ of a three-line scanner and ground points $A_1' \ldots A_3^{IV}$

As is shown in Figure 1, nets resulting from connections by rays between exposure stations and ground points can be spatially triangulated, but ties between the triangulation nets are loose. This consequence is only natural because the three-line scanner works lines by lines. Measures can be taken to circumvent the geometric weakness, for instance, by introducing non-parallel arrangements of the two outer CCDs (see Hofmann) or by providing more control information in form of GCPs.

In various research articles, polynomials are substituted for the time-related parameters. Mostly, only several polynomial coefficients are to be determined. If they fail to describe real variations of parameters which are often stochastic in nature, it is because polynomials are functional and merely suitable for expressions of global trends. To be able to handle local deviations, one should still estimate positions and attitudes at discrete stations separated by time intervals. It is very essential that an interpolation method is adopted to describe variations of parameters appearing between pre-selected stations. Linear models are practical and rather effective (compare Figure 2,) if the separation between two pre-selected stations is not large.

$$dx_{O_j} = (1-s/d)dx_{O_k} + (s/d)dx_{O_{k+1}} \qquad d\omega_j = (1-s/d)d\omega_k + (s/d)d\omega_{k+1}$$

$$dy_{O_j} = (1-s/d)dy_{O_k} + (s/d)dy_{O_{k+1}} \qquad d\varphi_j = (1-s/d)d\varphi_k + (s/d)d\varphi_{k+1}$$

$$dz_{O_j} = (1-s/d)dz_{O_k} + (s/d)dz_{O_{k+1}} \qquad d\kappa_j = (1-s/d)d\kappa_k + (s/d)d\kappa_{k+1}$$

A better model would then take more than two contiguous stations into account. Since the method of linear prediction (the method of linear least-squares interpolation, see Kraus and Mikhail) has been successfully applied in photogrammetry to analyses of discrepancies between given and calculated values, the present paper uses this interpolation method as models for the time-dependent parameters. The method itself is expressed as $s = \mathbf{c}^t \mathbf{C}^{-1} \mathbf{l}$,

where s = value to be interpolated
       $\mathbf{l}$ = column vector representing the values at reference points
       $\mathbf{c}$ = column vector containing covariances between point of interest and reference points
      $\mathbf{C}$ = symmetric matrix holding variances and covariances of reference points. Note that covariances are computed from (empirical) covariance functions which are Gaussian in most cases.

When used as models for parameters, it assumes the following forms:

$$dx_{O_j} = \mathbf{c}^t_{x_0} \mathbf{C}^{-1}_{x_0} dx_{O_k}$$

$$dy_{O_j} = \mathbf{c}^t_{y_0} \mathbf{C}^{-1}_{y_0} dy_{O_k}$$

$$dz_{O_j} = \mathbf{c}^t_{z_0} \mathbf{C}^{-1}_{z_0} dz_{O_k}$$

$$d\omega_j = \mathbf{c}^t_{\omega} \mathbf{C}^{-1}_{\omega} d\omega_k$$

$$d\varphi_j = \mathbf{c}^t_{\varphi} \mathbf{C}^{-1}_{\varphi} d\varphi_k$$

$$d\kappa_j = \mathbf{c}^t_{\kappa} \mathbf{C}^{-1}_{\kappa} d\kappa_k$$

As the models using the method of linear prediction are combined with collinearity conditions, the chain rule for partial derivatives is applied. The parameters related to the cycle number associated with any station O_j are all replaced by the parameters with the neighboring stations O_k's whose positions and attitudes are currently estimated, see the figure below. The number of O_k's stands for a correlation width which may be variable for each parameter.
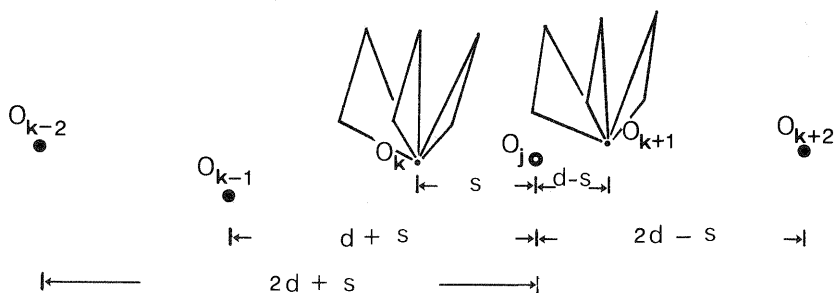

Figure 2. Exposure station O_j between the stations O_k's

Covariances are just functions of separations in line numbers providing correlation relations are independent of locations and directions. Once covariance functions are chosen, separations s, $d \pm s$ and $2d \pm s$ are set into the functions to form the covariance vectors and matrices which, by the way, can be readily multiplied with each other and stored sequentially for later repeated uses.

3. Geometric simulations

Our main objective is to study how effective modelling by the method of linear prediction is, in particular, regarding the number of GCPs. The known deviations of positions and attitudes from a nominal flight are illustrated in Figure 3. They are results from Fourier series with amplitudes and periods to be specified by a user. Variations of ω and κ indicate nutation effects and are more or less the same except a phase difference.
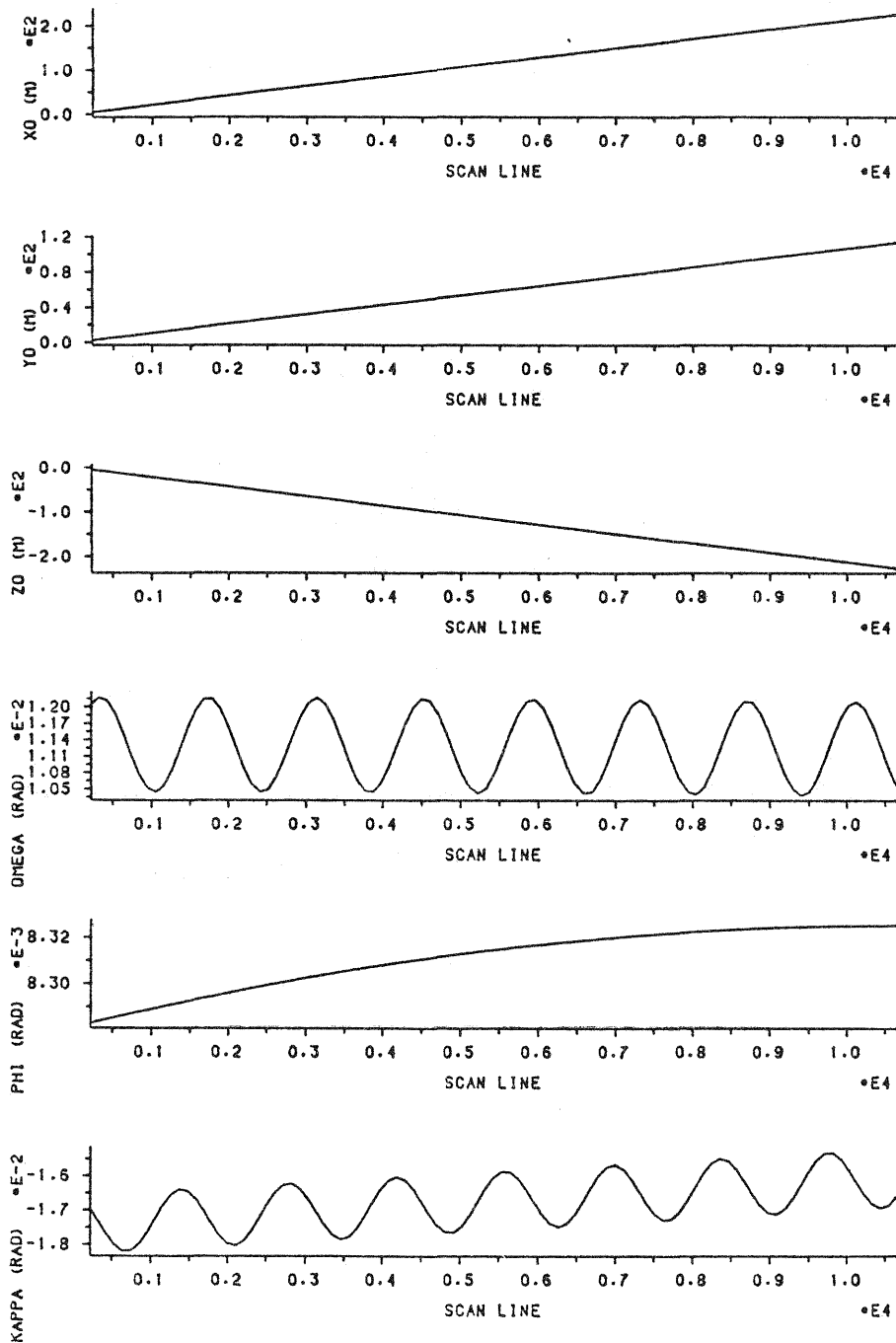
Figure 3. Given deviations of positions and attitudes for simulations

For geometric simulations, data about a three-line scanner such as MEOSS and about a terrain model are:

Camera focal length	61.1 mm
Flying altitude	420.0 km
Average scale of images	6867000.0
Size of a CCD-cell (in y)	0.010 mm
Field of view (in y)	31.9 deg
Angular resolution (IFOV in y)	0.164 mrad
1/2 convergence angle (1/2 FOV in x)	23.2 deg
Base to height ratio	0.43
Frequency of line scanning	104.87 Hz
Grid spacing in x (in object space)	10.0 km
Grid spacing in y	40.0 km
Number of grid points in x	73
Number of grid points in y	7
Total number of points on ground	511
Length of strip	720.0 km
Width of strip	240.0 km
Mean elevation of points above datum	0.45 km
Separation of exposure stations being estimated	20.0 km
Total number of stations being estimated	37
Total number of ground check points	508
Number of GCPs	3

Correlation widths for linear prediction models are all set equal to five (stations.) The time-referred positions and attitudes at the station O_j are expressed by those at its 5 contiguous stations O_{k-2}, O_{k-1}, O_k, O_{k+1}, O_{k+2}. From the following a priori root mean square errors for

Positions at exposure stations	±1400.0 m
Attitudes at exposure stations	±0.19 deg
Coordinates of GCPs	±30.0 m
Coordinates of image points in central imagery	±0.010 mm
Coordinates of image points in oblique imagery	±0.014 mm ,

weights are derived accordingly. Approximations for the x-, y-coordinates of ground points base upon an affine transformation. Approximations for z-coordinates are averages of the mean elevation and elevations from horizontal parallaxes of conjugate image points. The accuracy of approximations is ±80.02 m, ±375.47 m and ±500.70 m in x, y and z, respectively. The approximate values for positions and attitudes at the 37 exposure stations are prepared from the flight simulated. However, the estimation process makes use of the initial values only in conjunction with the above-mentioned weights.

Gaussian curves $c(d) = 0.9999 \cdot \exp(-k^2 \cdot d^2)$ are used as empirical covariance functions for the orientation parameters, because covariances are positive and decreasing in value when the separation d becomes larger. The index k for the measure of steepness is in average 0.00015 which is rather small but understandable since the deviations chosen for simulations are deterministic. Therefore, an empirical k (=0.00099) which incurs a smaller covariance as d increases is applied to the current case study. In other words, less correlation is allowed for the exposure stations to be estimated. Twelve iterations are needed until all non-linear collinearity conditions are numerically fulfilled (0.000008 as tolerance.)

For the purpose of knowing how accurate photogrammetric adjustments are, statistics are calculated from the differences between known and estimated information. There are 37 exposure stations along-track. Absolute maximum errors and root mean square errors of positions in meters and attitudes in degrees are listed below:

	x_O	y_O	z_O	ω	φ	κ
Abs.max.	58.48	65.48	54.34	0.056	0.008	0.060
RMSE	±23.82	±21.75	±24.39	±0.034	±0.003	±0.037

Coordinates in meters at 508 check points:

	x	y	z
Abs.max.	62.72	96.02	64.49
RMSE	±18.40	±37.37	±21.49

The quadratic mean out of x,y and z is ±27.1 m which is about two fifths of a pixel (69×69 m^2.) In addition, Figure 4 gives accuracy results at check points as functions of numbers of GCPs. Root mean square errors at ground check points show clearly that the models using the method of linear prediction are very effective indeed.
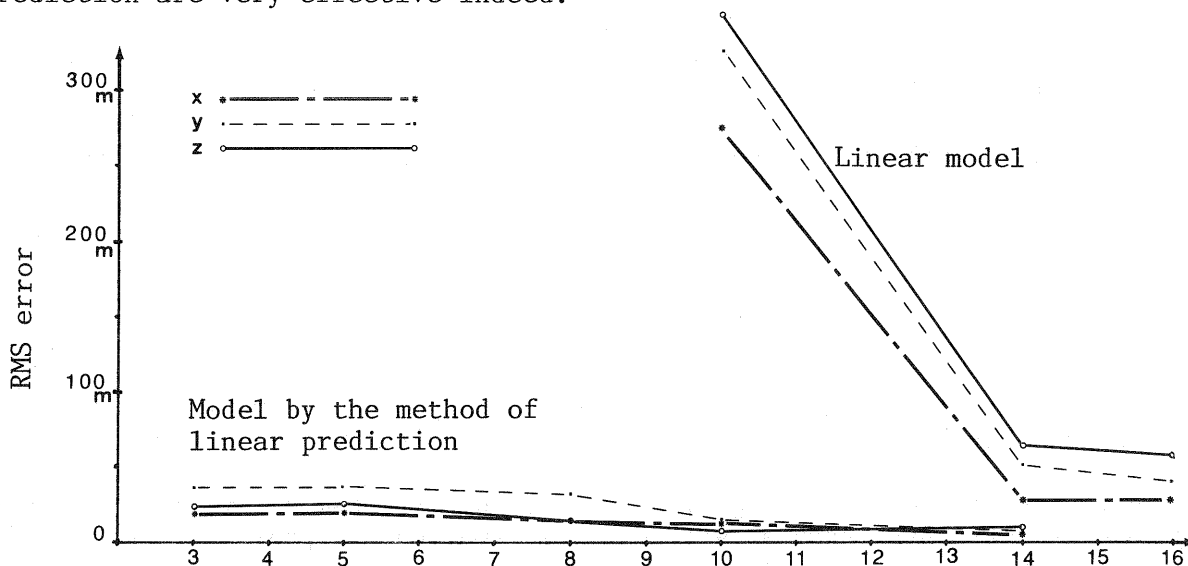

Figure 4. Accuracy at check points versus numbers of GCPs

4. Conclusions

It is well-known that photogrammetric strip adjustments are influenced by factors like:

- coordinates of image points correlated are differently precise
- whether correlated parameters are eliminated, or how they are weighted
- number and distribution of GCPs originating from different sources
- in cases of remotely sensed data, which model for the time-referred parameters of exterior orientation is selected.

In the present paper, emphasis has been laid upon the last factor. A well-tried interpolation method, the method of linear prediction as termed here, is directly used as models for time-dependent positions and attitudes at exposure stations. The original idea was to involve more than just two neighboring stations when it becomes necessary to consider image points whose exposure stations are others than those being estimated. The method of linear prediction has no restriction on the number of reference stations which may of course vary from case to case. If registrations of orientation parameters are available to users, covariance functions can be empirically determined. Then, the measure of steepness is referred to regarding the separation beyond which correlation plays only an insignificant role. In extreme cases, all stations being adjusted can be used as references points. Without real data, covariance functions are simply those from similar experiments.

In our research, levels of accuracy at check points exhibit no significant changes with respect to numbers of GCPs. When image data from three-line scanners can be evaluated to yield a great number of geometrically accurate points on the basis of the least reference, it is believed that the approach adopted is sound.

5. References

Aβmus, E. and Kraus, K.: Die Interpolation nach kleinsten Quadraten Prädiktionswerte simulierter Beispiele und ihre Genauigkeiten, Deutsche Geodätische Kommission bei der Bayerischen Akademie der Wissenschaften, Reihe A, No.76, 1974

Deutsche Forschungs- und Versuchsanstalt für Luft- und Raumfahrt e.V.: Monocular Electro Optical Stereo Scanner (MEOSS), Phase B Studie, 1984

Ebner, H. and Müller, F.: Processing of Digital Three Line Imagery Using a Generalized Model for Combined Point Determination, ISPRS Comm.III Symposium in Rovaniemi, 11 pages, 1986

Hofmann, O.: Dynamische Photogrammetrie, Bildmessung und Luftbildwesen 54(3), pp.105-121, 1986

Konecny, G. and Wu, J.: Analytische Streifen-Aerotriangulation für Stereo-Dreilinienabtaster, Bildmessung und Luftbildwesen 54(5), pp.179-194, 1986

Kraus, K. and Mikhail, E.M.: Linear Least-Squares Interpolation, XII. ISP Congress in Ottawa, Comm.III, 14 pages, 1972

Snyder, J.P.: Geometry of a Mapping Satellite, Photogrammetric Engineering and Remote Sensing 48(10), pp.1593-1602, 1982

Wu, J.: Investigation of Simulated MEOSS-Imagery for Sensor Navigation and Terrain Derivation, Proc. of the ISPRS Comm.I Symposium in Stuttgart, pp.279-284, 1986